10-23-1990

Collisional Excitation of CO by 2.3 eV H Atoms

George C. McBane
Grand Valley State University, mcbaneg@gvsu.edu

Scott H. Kable

Paul L. Houston

George C. Schatz
Northwestern University

Collisional excitation of CO by 2.3 eV H atoms

George C. McBane[a] Scott H. Kable, and Paul L. Houston
Department of Chemistry, Cornell University, Ithaca, New York 14853-1301

George C. Schatz
Depatment of Chemistry, Northwestern University, Evanston, Illinois 60208-3113

(Received 6 August 1990; accepted 23 October 1990)

Vibrational and rotational distributions of CO excited by collisions with 2.3 eV H atoms have been obtained by monitoring the products with vacuum ultraviolet (VUV) laser induced fluorescence. Translational-to-vibrational ($T \rightarrow V$) transfer is dominated by the dynamics of collisions occurring in the two wells on the H + CO potential energy surface, one characterizing the HCO radical and the other characterizing COH. The measured vibrational distributions agree well with the results of trajectory calculations performed on the *ab initio* potential energy surface of Bowman, Bittman, and Harding (BBH). The measured rotational distributions show two significant differences from the calculated ones. First, for $v = 0$ the experiments find more population in $J < 15$ than predicted. This discrepancy may be due to errors in the repulsive part of the BBH surface that is outside the HCO and COH wells, but inside the van der Waals well. Second, for $v = 1$, the experimental distribution is flat from $J = 0$ to $J = 10$, whereas the calculated one rises from near zero at $J = 0$ to a peak at $J = 12$. This discrepancy appears to be the result of an excessively high *ab initio* estimate (by a few tenths of an eV) of the barrier for H atom addition to CO to form COH.

I. INTRODUCTION

Scattering experiments have been the most sensitive probe of interparticle interactions available during this century. In chemical physics, gas-phase scattering has been used very profitably to explore interactions between atoms and molecules. The Born-Oppenheimer approximation is usually used to separate the theoretical description of the scattering process into two parts. The first is determination of the potential energy hypersurface, a function describing the dependence of the potential energy of the system on the nuclear positions. The second is the use of classical or quantum dynamics to model collisions on that surface. Both inelastic and reactive scattering processes can be studied, although reactive systems are more difficult because of the change in the natural coordinates of the problem and the usually large number of accessible product states.

Scattering experiments can provide initial data from which to generate a surface or act as tests of the accuracy of the surface and the dynamical technique. In atom-atom scattering, a well-developed procedure exists for inverting data from specialized experiments to obtain the potential function.[1-3] Even in this two-particle case, however, direct inversion of the data is quite involved and requires extensive data of very high quality. Most systems for which potentials are known from direct inversion of scattering data involve the rare gases or alkali metals.[4]

For molecular scattering, no rigorous inversion procedure is known. For collisions of atoms with molecules, or collisions between molecules, surfaces must be guessed or calculated; it is not yet possible to obtain the potential surface from scattering data alone. *Ab initio* quantum calculations at many geometries can be used to calculate a potential surface for some simple systems, and then spectroscopy and scattering data may be used to test and refine the surface.

An area of recent interest in atom-molecule scattering concerns collisions of fast hydrogen atoms with small molecules.[5] Calculated potential surfaces exist for several target molecules, including H_2,[6] O_2,[7] H_2O,[8] NO,[9] CO,[10] and CO_2.[11] Experimentally, the H atoms can be generated conveniently by photolysis of hydrides such as HBr, HI, and H_2S. The technique has the advantages that the H atoms are nearly monoenergetic and that the collisions occur at energies high enough to probe chemically interesting regions of the potential surface. Both inelastic and reactive scattering processes have been studied. The quantities measured experimentally are usually integral cross sections at various levels of state resolution, although differential cross sections have been obtained in at least one case.[12] The collisionally excited products have been detected by infrared fluorescence,[13-20] coherent anti-stokes Raman spectroscopy (CARS),[21] time-of-flight mass spectrometry,[12] and laser induced fluorescence.[22-24] Work in this field prior to 1987 was reviewed by Flynn and Weston.[5]

The H + CO system has been the subject of several experimental and theoretical investigations.[17-19,24-37] Interest in this particular system has been sparked by the availability of good *ab initio* calculations; a series of partial or global potential energy surfaces of increasing quality appeared over the past ten years.[10,28,30] The most complete and accurate surface available to date is the global surface

[a]Current Address: Department of Chemistry, University of Minnesota, Minneapolis, MN 55455.

of Bowman, Bittman, and Harding (the BBH surface).[10] Trajectory calculations performed on this surface have been used to describe high-energy scattering,[24,31] and several quantal studies have examined resonances.[32–36] Recently a time-correlation function approach was applied by Micha *et al.* to H + CO scattering at 1.6 eV.[37]

In an earlier paper, we reported measurements of rotationally resolved integral cross sections for collisional excitation of CO by 1.6 eV H atoms and compared them with trajectory calculations performed using the BBH surface.[24] In that paper the primary conclusion was that the most effective collision geometry for vibrational excitation of the CO was approach of the H atom through the HCO well, followed by direct scattering from the hard repulsive inner wall of the well. In this work, results from 2.3 eV collision experiments are presented. At 2.3 eV, the collision energy is high enough for the H atom to cross the saddle point into the HOC well, a region not accessible at 1.6 eV. The vibrational populations of CO after collision with 2.3 eV H atoms were previously measured by Flynn *et al.* and by Leone *et al.*, using infrared fluorescence.[17–19] We have obtained rotationally state-resolved populations for the $v = 0$, 1, and 2 levels and have interpreted the results both through surprisal analysis and by comparison with trajectory calculations on the BBH surface.

II. EXPERIMENTAL

The experiments were performed by expanding a mixture of CO and H_2S in a supersonic free jet. Hydrogen atoms ($E_T \sim 2.3$ eV) produced by dissociation of the H_2S with an ultraviolet laser pulse collided with the CO, which was detected 75 ns later using vacuum ultraviolet laser-induced fluorescence. Details are provided below.

A. Gas mixtures

An aluminum cylinder of UHP grade CO was obtained from Matheson. This source of CO was tested by mass spectrometry and found to be free of carbonyl and water impurities. Samples were prepared by filling aluminum cylinders with pure CO to 92% of the desired total pressure and adding H_2S. For measurements of vibrationally elastic cross sections to states of CO with $J < \sim 15$, the thermal population of CO was too large to allow extraction of collisionally excited populations. For these experiments, a seeded mixture of 1% CO and 1% H_2S in argon was used.

B. Molecular beam parameters

The gas mixtures were expanded from a pressure of 2 atm through a pulsed nozzle (Newport BV-100 operating at 10 Hz) with a 0.5 mm orifice. The CO rotational temperature in the experiments using 92% CO was measured to be about 35 K; the most highly populated rotational level at that temperature is $J = 2$. In the experiments performed with 1% CO/1% H_2S mixtures in argon, the CO rotational temperature in the beam was about 4 K, where the most highly populated rotational level is $J = 0$.

C. Photolysis laser

The H_2S was dissociated with pulses from an ArF excimer laser (Lambda Physik EMG-101), telescoped to a collimated beam about 4 mm wide and 5 mm high in the center of the molecular beam chamber. The pulse energy inside the beam chamber was about 10 mJ, the pulse width was 10 ns, and the dissociation beam crossed the free jet 12 mm below the nozzle. Using an H_2S absorption cross section[38] of 6.4×10^{-18} cm^2, we calculate production of about 4×10^{14} hydrogen atoms per pulse. The transmitted 193 nm beam struck a cell filled with Rhodamine 6G dye, and fluorescence from the cell was monitored with a photodiode and used to normalize the laser-induced fluorescence (LIF) signals.

D. VUV laser

The collisionally produced distribution of internal states of CO was probed with LIF, using a vacuum ultraviolet (VUV) beam at right angles to both the free jet and the dissociation laser. The apparatus for generation of tunable coherent VUV light by four-wave sum mixing has been described in previous publications.[39–43] Briefly, the beams from two pulsed dye lasers (Lambda Physik FL2000E) pumped by a dual-cavity XeCl laser (Lambda Physik EMG 150ES) were combined in magnesium vapor, where four-wave mixing produced the output frequency $2\omega_1 + \omega_2$. The ω_1 dye laser typically produced 5–8 mJ of light in an 8 ns pulse; the ω_2 laser, pumped by the stronger "amplifier" cavity of the excimer laser, produced between 8 and 25 mJ. The polarization of one of the beams was rotated 90° with a half-wave plate, and the two beams were combined in a Glan-Taylor prism. They subsequently passed through a quarter-wave plate, which made them circularly polarized in opposite senses, and were focused via a 250 mm lens into a heat pipe containing 30 Torr of magnesium vapor. The weaker laser was tuned to 430.8 nm in order to excite the $3s^2 \rightarrow 3s3d$ two-photon transition in magnesium; the other laser could be tuned over a wide range of wavelengths to provide output from 140 to 175 nm.

The VUV output was collimated with an MgF_2 lens and sent via an evacuated tube to the molecular beam vacuum chamber. The transmitted intensity was monitored with a solar-blind photomultiplier (EMI G-26E314LF) and used to normalize the CO LIF signals.

An important modification of the heat pipe contributed to the convenience of these experiments. Addition of lithium metal to the heat pipe prevents Mg crystal growth near the windows, extending the useful life of the heat pipe from several hours to several months. The lithium does not interfere with VUV production over most of the useful range of the instrument, although a few sharp anomalies have been noticed and attributed to Li absorption.

E. Signal detection

CO fluorescence following excitation of the $A\,^1\Pi \leftarrow X\,^1\Sigma^+$ transition was collected by a 1.5 in. f/1 lens oriented 45° to both laser beams. It passed through a filter

(Acton 193-FR on MgF_2) to remove 193 nm scattered light and was detected by a second solar-blind PMT (EMR 542G-09-17). The VUV laser was fired, and the fluorescence collected, 75 ns after the photolysis. It was not easy to use a shorter delay because the photomultiplier took about 50 ns to recover from fluorescence produced by a multiphoton process involving the 193 nm beam, which apparently produced a significant CO ($A\ ^1\Pi$) population. The LIF signals were amplified in a 10x preamplifier (LeCroy VV100B) and averaged with a gated integrator (Stanford SR250). A set of power-dependence experiments was performed during each experimental session to establish that the signals being collected were linear in each of the VUV and 193 nm intensity.

When it was necessary to eliminate contributions from thermally excited CO, the dissociation laser was fired on every other pulse and active baseline subtraction was used. The data were collected on a DEC PDP-11 computer, and analyzed on an IBM PS/2 Model 70 or Model 80 computer.

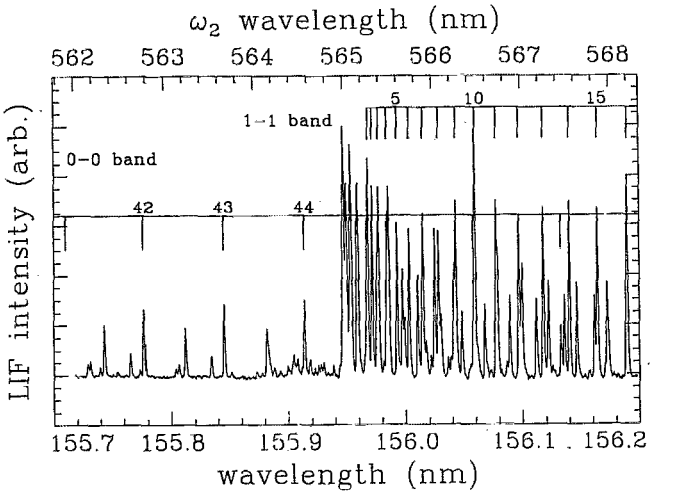

FIG. 1. Region of the experimental spectrum showing high-J lines of the (0,0) band and the (1,1) bandhead. Q-branch transitions are identified in the figure. The (4,3) bandhead is also just observable near the $Q(44)$ line of the 0–0 band.

III. RESULTS

A. Control experiments

The effect of clustering on experiments in the pure CO expansion was determined to be insubstantial in our earlier work on 1.6 eV collisions.[24] We have performed a similar check on the results from the Ar-cooled expansions. To test the effects of clustering in the free jet, two scans were taken using the seeded sample at backing pressures of 1.3 and 3.3 atm. Since the probability of forming clusters should vary at least as the square of the density of molecules in the throat of the jet, the clustering conditions in these two scans should differ by at least a factor of 6. Because we found no consistent difference between the two scans, we concluded that collisions of H atoms with $(CO)_n$, $(CO)_m(Ar)_n$, or $(CO)_m(H_2S)_n$ clusters do not affect the results.

It is also conceivable that collisions *inside* $(H_2S)_m(CO)_n$ clusters could have a discernible effect. For example, Wittig and co-workers have used clusters of H_2S with CO_2 to study oriented collisions.[44] Collisions inside such clusters, however, produce scattered CO immediately after the photolysis pulse, whereas the signals we observed showed a linear time dependence whose extrapolated intercept was nearly zero.

B. Populations

We recorded fluorescence excitation spectra for the $(v',v=v'')$ (Ref. 45) = (0,0), (1,1), (2,2), (0,1), and (0,2) bands of the $A \leftarrow X$ transition of scattered CO. The high-J'' part of the (0,0) band and the bandhead of the (1,1) band are shown in Fig. 1. We also recorded the bandhead regions of the (2,3) and (4,4) bands in order to provide estimates of the population in higher v states. For the $v''=0$, 1, and 2 levels, the P, Q, and R branches for each band provide several independent determinations of the population in each rotational level. Typically, we made from 4 to 10 measurements of the population in a particular (v'',J'') state. The redundancy permits statistical estimates of measurement errors.

The lines were assigned using the molecular constants of Guelachvili *et al.*[46] for the X state and Field *et. al.*[47,48] for the A state. The overlaps of the three main bands provide a convenient means for relative intensity calibration, so that comparisons of integrated vibrational populations may be made. Since the linewidth is dominated by the 0.6 cm^{-1} spectral width of the exciting light, the amplitude of any single line is proportional to its integrated intensity. The measured amplitudes were inverted to obtain populations using the formula

$$I(v'J' \leftarrow v''J'') \propto \nu \mu_{el}^2 S_{J'J''} q_{v'v''} N_{v''J''} F(v')/g(J''), \qquad (1)$$

where $I(v'J' \leftarrow v''J'')$ is the fluorescence intensity of the line, ν is the excitation frequency, μ_{el}^2 is the square magnitude of the electronic transition moment, $S_{J'J''}$ is the Hönl–London factor,[49] $q_{v'v''}$, is the Franck–Condon factor for the excitation,[50] $N_{v''J''}$ is the population in the v'', J'' level, $F(v')$ is the instrument sensitivity function for detecting fluorescence from the v' level, and $g(J'')$ is the degeneracy of the J'' level. Tables of fractional $A^1\Pi$ character[47,48] were used to correct for variations in μ_{el}^2. The sensitivity function $F(v')$ corrects for the frequency dependencies of the 193 nm filter transmission and the photomultiplier quantum efficiency. It is given by the formula

$$F(v') = \sum_{v'''=0}^{\infty} q_{v'v'''} QE(v',v''') T(v',v'''), \qquad (2)$$

where $q_{v'v'''}$ is the Franck–Condon factor for the emission step, $QE(v',v''')$ is the quantum efficiency of the PMT at the emission frequency from v' into v''', and $T(v',v''')$ is the fraction of light transmitted by the 193 nm filter at that frequency. The frequency dependencies are sufficiently smooth that the J' dependence can be ignored, and the sum can be truncated at low v because the Franck–Condon

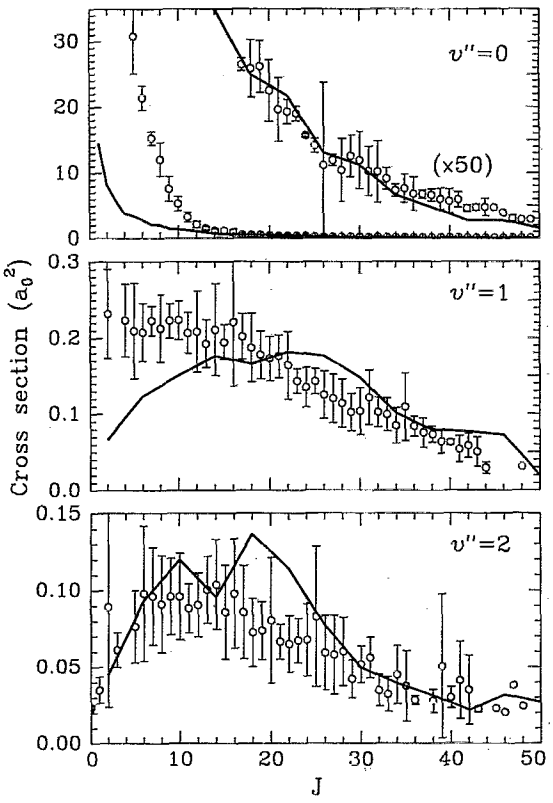

FIG. 2. Relative populations for $v=0$, 1, and 2 scattered CO. Error bars give 80% confidence limits calculated from multiple measurements; points without bars were measured only once. The Circles give experimental measurements, while the solid line gives the result predicted by the classical trajectory calculations. The experiments were scaled to the theoretical cross sections over the range $v=0$, $J>16$, as shown in the expansion. The experimental results for $v=1$ and 2 were scaled using the same factor as for $v=0$.

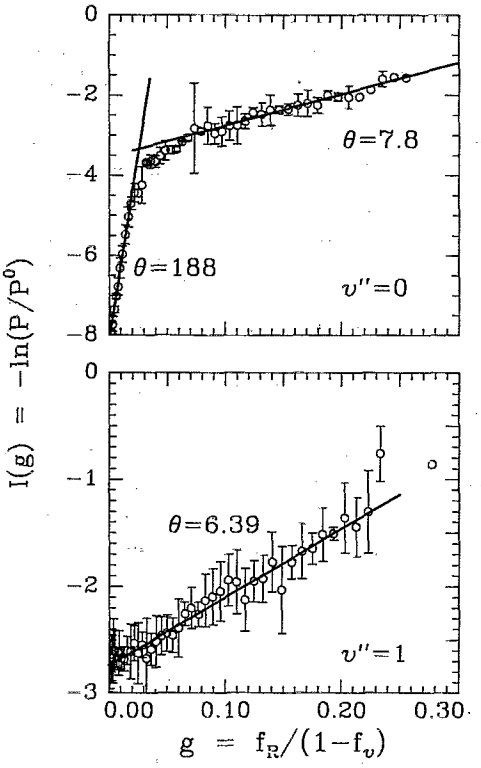

FIG. 3. Surprisal plots for $v=0$ and $v=1$. The fitted lines were obtained from least-squares fits weighted by the uncertainties for each point.

factors rapidly become small. We have calculated the instrument sensitivity function using manufacturer-supplied frequency response curves for the PMT and filter.

The temporal gate width of our detection apparatus was set wide enough ($\sim$30 ns) that variations in the fluorescence lifetimes of different emitting states did not affect the measurement.

The data were collected in many separate scans over short wavelength ranges. The relative scale factors were determined by minimizing the quantity

$$\sum_i (P_{v'',J''}(i) - P_{v'',J''}(\text{mean}))^2/P_{v'',J''}(\text{mean})^2 \qquad (3)$$

summed over all vibrational and rotational levels. Here $P_{v'',J''}(i)$ indicates the i^{th} measurement of the relative population of level (v'',J'').

The populations obtained from our data are shown in Fig. 2 for $v''=0$, 1, and 2. The average of all measurements for each level is plotted, with error bars representing 80% confidence limits. The spectra which determine populations for the $J''\leqslant 17$ part of the ground vibrational state were taken with samples of CO and H_2S seeded in argon. The results of the seeded and unseeded experiments were identical in the region of overlap between $J''=10$ and $J''=21$.

C. Surprisal analysis

In order to present the results more compactly and to determine how many constraints control the data, we have performed an information–theoretic analysis of the data. In this analysis the data is compared to a statistical "prior" distribution in which available energy is distributed solely on the basis of the density of states. The prior distribution of rotational energy between an atom and a diatomic molecule is given in the rigid rotor-harmonic oscillator approximation by[51]

$$P^0(f_R|f_v)=(3/2)(1-g)^{1/2}/(1-f_v), \qquad (4)$$

where f_v is the fraction of the total energy appearing in vibration, f_R is the fraction of total energy appearing in rotation, and g is the reduced rotational energy variable $f_R/(1-f_v)$. The surprisal for a particular value of g is defined as

$$I(g)=-\ln\,(P(g)/P^0(g)), \qquad (5)$$

where $P(g)$ is the observed probability of having final reduced rotational energy g. Plots of $I(g)$ vs g for $v=0$ and 1 are shown in Fig. 3. The plot for $v=0$ is clearly bilinear. The points with $g<0.02$ describe a line with slope 187.5 ± 5.4, while the points with $g>0.054$ describe a line with slope 7.84 ± 0.25. For the $v=1$ data, most of the

points lie on a line with slope 6.39 ± 0.37. (For purposes of extrapolation of vibrational populations, the points in $v=1$ with $g<0.02$ were described by a line with slope -0.69, but the deviations of those points from the primary line are not statistically significant. The uncertainties listed are one standard deviation.) All the slopes are derived from least-squares fits weighted by the sample standard deviations of the data points, and the goodness-of-fit parameters were calculated to establish accuracy of the linear models.

The surprisal analysis was used to extrapolate population data into regions where no measurements were made in order to estimate total vibrational populations. Propagation of error was used to provide error estimates for the vibrational populations. The extrapolation from $J=4$ to $J=1$ in $v=0$ is by far the greatest contributor to the uncertainty in the vibrational populations, since it contributes over 40% of the total $v=0$ population. For this reason, relative populations in $v=0$ with $J \geqslant 10$ as well as total relative populations are reported here. For $v=3$ and 4, signal levels did not permit determination of rotational distributions; estimates of the total populations in those levels were obtained from measurements of intensities at the bandheads. The relative vibrational populations, normalized to $v=1$, are (37.2 ± 1.3; 3.2 ± 0.1 for $J \geqslant 10$), (1.00 ± 0.02), (0.42 ± 0.01), (0.11), and (0.08) for v of 0, 1, 2, 3, and 4, respectively. The quoted uncertainties represent one standard deviation from the linear surprisal fits. For the $v=3$ and 4 populations, the values given are obtained from measurements of the bandhead heights and should be considered rough estimates. [A similar estimate of the $(v=1)/(v=2)$ ratio was in error by 15%.]

IV. DISCUSSION

A. Speed distribution of H atoms

To establish that the differences between measured cross sections and the calculated ones to be described below are not artifactual, we have considered two possible experimental causes of the differences: clusters in the molecular beam and slow H atoms from the dissociation or from multiple collisions. A discussion of the problem of clusters was given above. The probable speed distribution of the H atoms and its effect will be discussed here.

The 193 nm photodissociation of hydrogen sulfide has been studied by several groups.[52–54] Very little of the available energy appears as rotational excitation of the HS fragment. Xu *et al.*[53] and Xie *et al.*[54] have made recent measurements of the translational energy distribution of the H atoms; their results show that roughly 62–68 % of the H atoms are produced along with $v=0$ HS fragments, and so have 2.3 eV translational energy. The remainder of the H atoms are produced in conjunction with HS fragments in vibrational levels ranging from 1 to 8, with the $v \leqslant 4$ levels predominating. Since the H atoms have time to make more than one collision before the LIF probe, the effective energy distribution is not as sharp as the original. We have determined the actual distribution of H atom energies which produced the observed CO excitation by measuring the Doppler profile of H atoms produced by photolysis of H_2S under conditions identical to those used for our study. Frequency tripling of light near 365 nm in krypton was used in order to detect the H atoms by laser-induced fluorescence on the Lyman-α line. Analysis of the Doppler profile scanned with an etalon in the Lambda Physik dye laser confirmed a hard-sphere calculation indicating that over 50% of the collisions occur with energies above 2.0 eV for both the neat and seeded expansions.

B. Comparison with trajectory calculations

We now compare the experimental results with the results of classical trajectory calculations performed on the BBH potential surface. The calculations were similar to ones reported in our earlier paper on 1.6 eV scattering, the only differences being the higher collision energy and a larger maximum impact parameter necessary to ensure convergence of the low-J cross sections (8.0 vs 4.01 Bohr).

Since the experiments determined only relative cross sections, it was necessary to scale the results for comparison with the trajectory calculations; the scale factor was chosen to provide good overlap in the $18 \leqslant J \leqslant 50$ region of the $v=0$ rotational distribution. The measured populations are shown overlaid on the trajectory results in Fig. 2. The statistical uncertainty in the calculated cross sections is 30% for cross sections of 0.1 a.u. and 10% for 1.0 a.u. The uncertainty varies as the square root of the cross section and is roughly equal to the experimental uncertainty. In general, the calculated rotational distributions agree quite well with the data for $J>15$ in $v=0$ and for $J>10$ in $v=1$, and for all of $v=2$. The most obvious difference is the very sharp peak in cross section in the experimental results for $J<15$, $v=0$. At $J=5$ the experimental cross section is roughly four times the calculated one. For $v=1$, the cross section as a function of J is roughly flat from $J=0$ to 12 in the experimental results, while it drops off below $J=15$ in the calculations.

1. Rotational distribution in $v=0$

The sharp peak at low J in the observed $v=0$ cross sections is the most dramatic observation in the experiment; the probability of transferring between 40 and 500 cm^{-1} of energy is about 15 times larger than that of transferring more than 500 cm^{-1}. The low J cross sections are also the most serious source of disagreement between theory and experiment (Fig. 2), so it is relevant to consider the mechanism for producing these states and possible explanations for the disagreement between theory and experiment. An important conclusion from our trajectory calculations is that collisions producing $J \leqslant 20$, in general, and $3 \leqslant \Delta J \leqslant 10$, in particular, do not have their turning points in the van der Waals well region. The turning point here is defined as the position of closest approach between the H atom and the CO center of mass. We find that the H-CO distance at the turning point of each trajectory which leads to $3 \leqslant \Delta J \leqslant 10$ is always less than 5.0 a_0 and usually closer to 4 a_0. Such collisions sample interaction potentials that are always above 0.2 eV.

Although the BBH surface has been globally determined, it does not treat the van der Waals well region or

beyond accurately. However, given the range of inner turning points sampled by collisions producing $3 \leqslant \Delta J \leqslant 10$, it is not obvious that errors in the van der Waals regions are significant. We conclude that the only way that the BBH surface could be the origin of the discrepancy between theory and experiment is if the fit is defective in the 4–5 a_0 region, where trajectories producing $3 \leqslant \Delta J \leqslant 10$ have inner turning points.

There could be a number of experimental sources for the discrepancy between theory and experiment in the low J region for $v = 0$. Multiple collisions of the excited CO molecules with other species present must certainly be considered, but we calculate that fewer than 15% of the excited CO target molecules experience a second hard-sphere collision with Ar before detection. The distribution of H atom energies mentioned above, arising from precursor photodissociations and from multiple collisions of the H atom with different CO molecules, must also be considered. However we can eliminate this as a contributing cause by two different arguments. First, about 25% of the excitations in the Ar-seeded experiment occur in collisions with energies less than 1.6 eV. The population of excited CO in $v = 0$, $J \leqslant 10$ is more than 85% of the total collisionally excited population, so it certainly was not created solely by collisions with those slow atoms. Second, if slow H atoms rather than deficiencies in the potential energy surface were responsible for the discrepancy, then one would expect trajectory calculations performed at lower energies such as 1.6 eV to exhibit features similar to those observed here.[55] Calculations done for 1.6 eV H atoms are reported in our earlier paper.[24] We have now extended these to large impact parameters and to other energies between 1.0 and 2.3 eV. The calculated cross sections for $\Delta J < 10$ are very similar to those calculated at 2.3 eV. The possibility of Ar–CO clusters as targets producing primarily low-J CO product remains the most likely experimental cause of the discrepancy, although the failure to detect evidence for this mechanism in pressure-dependence experiments is a strong argument against it.

2. Rotational distribution for $v=1$

In our earlier work on H + CO at 1.6 eV, we found excellent agreement between the results of the trajectory calculations and the data for the rotational distribution in $v = 1$. By examining the locations of the turning points for trajectories which excited $v = 1$, we concluded that the most efficient mechanism for vibrational excitation was collision with the hard repulsive wall inside the HCO well. Those collisions are effective at impulsively exciting the CO vibration; because of the geometry in the HCO well and the steep repulsive character of the inner wall, they tend also to excite high rotational levels. The $v = 1$ rotational distribution from 1.6 eV collisions is peaked at roughly $J = 15$, and falls toward zero at lower J.

The trajectory results for 2.3 eV collisions show a similar trend; nearly all the vibrationally inelastic collisions have turning points inside the HCO well. However, a few $v = 1$ CO products are formed from collisions at the oxygen end near the HOC well. Between the HOC saddle point and the HOC well, the CO distance of minimum energy increases from 2.1 to 2.4 Å. This relaxation of the CO internuclear distance, corresponding to a partial breaking of the C≡O triple bond, provides a strong coupling to CO vibration for those trajectories which cross the HOC saddle point. Since the collisions are much "softer" and the trajectories are directed more toward the center of mass of the CO than in collisions in the HCO well, these O-end encounters produce much less rotational excitation. Figure 4 overlays turning points of trajectories which produced $v = 1$ CO on a contour plot of the BBH surface at a C–O distance of 2.1 Å. Turning points of trajectories which produced final J values of $\leqslant 20$ are shown as open circles, while those producing $J \geqslant 20$ are shown as filled triangles. It is clear that a much larger fraction of the vibrationally inelastic collisions which pass through the HOC well produce low final J.

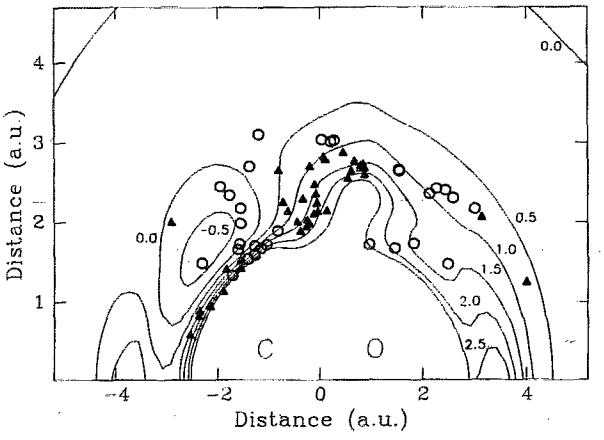

FIG. 4. Contour plot of the BBH potential surface with turning points of trajectories which produced $v = 1$. Open circles represent turning points (points of closest approach to the CO center of mass) for trajectories which produced final J values between 0 and 20, while solid triangles are for final J values exceeding $J = 20$. The contour interval is 0.5 eV.

The data for 2.3 eV collisions provide a rotational distribution in $v = 1$ which is nearly flat from $J = 0$ to $J = 10$ and then falls off slowly at higher J, in contrast to the 1.6 eV results which were peaked at $J = 15$. We interpret this qualitative change to reflect the appearance of a second mechanism for vibrational excitation, namely collisions which pass over the HOC saddle point. At 2.3 eV, many more H atoms are able to climb the high wall to the saddle point, an unlikely event at 1.6 eV. Those vibrationally inelastic collisions at the oxygen end of the molecule contribute population in low rotational levels.

The trajectory calculations do not match the observed distribution for low J in $v = 1$. The discrepancy is probably due to an inaccurate description of the HOC saddle point region on the BBH surface. When the surface was generated, spectroscopic data on HCO (Refs. 56 and 57) were

used to adjust the surface in the HCO well region. No data were available on HOC, so the surface in that region was fit to the unadjusted *ab initio* energies. Those energies are probably a little ($\sim$.2 eV) too high, so in the trajectory calculations it is a little too hard for trajectories to sample the HOC well region. Indeed, lowering the barrier to the COH well by 0.2–0.4 eV resulted in enhanced cross sections for low J ($J<5$) without changing the cross sections for larger J.

It is unlikely that the difference between calculated and observed low-J, $v=1$ cross sections is caused by the slower H atoms discussed above for two reasons. First, the probability of vibrationally inelastic collisions drops off rapidly as the collision energy decreases, so that the number of $v=1$ molecules produced by slow ($E\lesssim$ 1.5 eV) atoms should be much smaller than the number produced by the faster atoms. Second, the flat cross section at low J was not seen in the 1.6 eV work, where all the atoms are slower; the distribution seen in that experiment rose from $J=0$ to $J=13$. The change in rotational contour as the mean speed of the H atoms increases is very probably the result of a new channel available at the higher collision energy.

3. Rotational distribution for v=2

In the 1.6 eV work, it was found that the cross section ratio for excitation of $v=2$ vs $v=1$ was $\sigma(v=2)/\sigma(v=1)=0.1$. At 2.3 eV, however, the $\sigma(v=2)/\sigma(v=1)$ ratio increases to roughly 0.42. Even at 2.3 eV, essentially the only mechanism available to excite CO to $v=2$ is collision inside the HCO well. The rotational distribution rises from nearly zero at $J=0$ to a maximum near $J=11$, then decreases slowly at higher J. Such a distribution is expected for collisions inside the HCO well; it is very much like the one seen for $v=1$ in the 1.6 eV experiment. The trajectory results reproduce the data quite well (Fig. 2), reflecting the high accuracy of the BBH surface in the HCO region. Nearly all the turning points for trajectories producing $v=2$ occur in the HCO well.

4. Vibrational distribution

It is gratifying to note that the trajectory calculations predict the overall efficiency of vibrational energy transfer well. All of the data in Fig. 2 were scaled by the same factor, so the agreement between the data and the trajectory results for $v=1$ and $v=2$ indicates the accuracy of the predictions of $T\rightarrow V$ transfer. The inaccuracies which appear are those at low J in $v=0$ and 1, whose causes were discussed above. The agreement in $T\rightarrow V$ transfer efficiency reassures us that we have scaled the data appropriately by using the high-J section of the $v=0$ rotational distribution.

The cross sections for excitation into $v=3$ and 4 are subject to considerable uncertainty in both the calculation and the experiment. The theoretical ratio for the cross sections for excitation into $v=2$:3:4 is 0.42: 0.11: 0.04, while the experimentally obtained ratio is 0.42: 0.11: 0.08. The agreement for $v=3$ is probably fortuitous, because the experimental value is uncertain by at least 30%. Given the very small total cross sections into these vibrational levels, a disagreement of a factor of 2 for the $v=4$ cross section is not very disappointing.

We can also compare our vibrational distribution to that obtained by Wight and Leone.[19] For a collision energy of 2.3 eV, they obtained a distribution for $v=1$:2:3:4 of 1.00: 0.20: 0.11: 0.013. Our results give a distribution for these vibrational levels of 1.00: 0.42: 0.11: 0.08. Thus, although there is substantial agreement between the two experiments, we observe more population in $v=2$.

It is interesting to note that the cross sections for production of vibrationally excited products are larger in the case of H + CO than, for example, in the case of H + CO_2. The ratio of $CO(v=1)/CO(v=2)$ is about 2 based on our work, whereas at the same collision energy the ratio of $CO_2(001)/CO_2(002)$ is about 13 based on the work of O'Neill *et al.*[58] This difference may be the result the larger attractive well in H + CO as compared to H + CO_2 However, it is important to note that the effect of the well is not to induce complex formation at these energies, but rather to increase the effective translational energy and, perhaps, to make the potential steeper at the inner turning point. The effect of attractive forces has also been discussed by Wight and Leone in comparing the H + CO to H + NO vibrational excitation.[19] These authors attributed the weaker energy dependence of the H + NO vibrational excitation to the fact that the H + NO potential energy surface has a wider and deeper well.

V. CONCLUSIONS

Several detailed observations about the dynamics of H + CO scattering have been made. Most striking is the information gained from examining rotational distributions in vibrationally inelastic scattering. $T\rightarrow V$ transfer between H and CO at 2.3 eV is dominated by dynamics occurring in the two wells on the HCO surface.

The HCO well, which corresponds to a bound HCO molecule, is more important; the great majority of vibrationally inelastic trajectories pass through this well. The HCO well provides the easiest approach for an H atom to the regions of the surface where it can impart a significant impulsive force on the CO oscillator, but the basic character of the CO triple bond remains essentially unchanged during the collision.

The COH well, on the other hand, can be reached only by crossing a high barrier. The potential is not as steep on the inner wall of the COH well as it is in the HCO well, but the COH radical has a much longer CO bond at its minimum-energy configuration. The change in equilibrium bond length as the H atom moves from the COH saddle point to the COH well provides strong coupling to higher vibrational states, without a strong tendency to excite high rotational levels. Since the barrier to COH formation is high, vibrationally inelastic collisions at the O end of the molecule are more important for the 2.3 eV H atoms than for the 1.6 eV H atoms studied previously.

The BBH surface describes H + CO scattering in the region of the HCO well very accurately. This accuracy is reflected in the good agreement between calculated and observed relative vibrational cross sections for $v\geq 1$, and

rotational distributions for $v = 2$ and for the high-J part of $v = 1$. However, the contribution of collisions in the COH well at 2.3 eV is underestimated in trajectories on the BBH surface. The COH saddle point is probably a little too high on this surface, so that fewer trajectories can access the region between the saddle point and the well to produce vibrational excitation.

There is also a discrepancy between theory and experiment with regard to the cross sections for low J states in vibrationally-elastic scattering. This could be due to an error in the BBH surface, but if it is, it would have to be associated with geometries where the *ab initio* calculations should have been accurate.

Several experiments could provide still more information on the dynamics of H + CO collisions. Repeating the present work using D_2S rather than H_2S should probe the dependence of the cross sections on the relative velocity or momentum of the collision partners, without changing the collision energy substantially. (In vibrationally inelastic scattering of He from CO, the transfer was found to be velocity-dependent rather than momentum-dependent.[59]) Such an experiment might yield information on the steepness of the repulsive wall in the HCO well and the force on the CO bond in the repulsive region.

The experiment presented here detected no quantum effects in H + CO scattering. Bowman *et al.*[32–35] and Geiger and Schatz[36] have predicted resonances in the scattering in the region of the HOC bound-state energies. It should be possible to observe these H + CO resonances by monitoring the population of a single high-J level of scattered CO as the photolysis wavelength is scanned. Two technical problems arise in such an experiment. The first is the change in the dissociation cross section as the photolysis wavelength is changed. However, the resonances are expected to be narrow enough to make that change unimportant. The second is the spread in H-atom velocities. In our experiment that spread has two sources: the initial distribution caused by the internal excitation of the HS fragment in the dissociation and the spread caused by multiple collisions of the H atoms. The energy distribution problem could probably be circumvented by using a different precursor and by using beam densities low enough or delay times short enough to attain single-collision conditions for the H atoms. Determination of resonance energies in the scattering would provide very accurate information on the locations of vibrational levels in the metastable COH molecule. This radical has not yet been observed spectroscopically, although it is possible that the recently resolved HCO $\tilde{B}$-state fluorescence[60,61] probes some of these regions.

ACKNOWLEDGMENTS

This work at Cornell was supported by the Air Force Office of Scientific Research under Grant No. AFOSR-89-0162. We would like to acknowledge Dr. G. K. Chawla for initial experimental work and Dr. C. E. M. Strauss and Professor George Flynn for helpful discussions. G. C. S. acknowledges financial support from NSF Grant No. 8715581 and helpful conversations with L. B. Harding. We gratefully acknowledge Dr. D. Crosley for providing a preprint of Ref. 60 and X. Zhao for providing a preprint of Ref. 61.

[1] O. B. Firzov, Zh. Exp. Teor. Fiz. **24**, 279 (1953).
[2] W. H. Miller, J. Chem. Phys. **51**, 3631 (1969).
[3] T. J. P. O'Brien and R. B. Bernstein, J. Chem. Phys. **51**, 5112 (1969).
[4] R. J. Cross, Acc. Chem. Res. **8**, 225 (1975), and references therein.
[5] G. W. Flynn and R. E. Weston, Annu. Rev. Phys. Chem. **37**, 551 (1986).
[6] (a) P. Siegbahn and B. Liu, J. Chem. Phys. **68**, 2457 (1978), (b) D. G. Truhlar and C. G. Horowitz, *ibid* **68**, 2466 (1978); **71**, 154 (1979).
[7] C. F. Melius and R. J. Blint, Chem. Phys. Lett. **64**, 183 (1979).
[8] G. C. Schatz and H. Elgersma, Chem. Phys. Lett. **73**, 21 (1980).
[9] M. C. Colton and G. C. Schatz, J. Chem. Phys. **83**, 3413 (1985).
[10] J. M. Bowman, J. S. Bittman, and L. B. Harding, J. Chem. Phys. **85**, 911 (1986).
[11] G. C. Schatz, M. S. Fitzcharles, and L. B. Harding, Faraday Disc. Chem. Soc. **84**, 359 (1987).
[12] S. A. Buntin, C. F. Geise, and W. R. Gentry, J. Chem. Phys. **87**, 1443 (1987).
[13] C. R. Quick, R. E. Weston, Jr., and G. W. Flynn, Chem. Phys. Lett. **83**, 15 (1981).
[14] F. Magnotta, D. J. Nesbitt, and S. R. Leone, Chem. Phys. Lett. **83**, 21 (1981).
[15] C. A. Wight, F. Magnotta, and S. R. Leone, J. Chem. Phys. **81**, 3951 (1984).
[16] S. Datta, R. E. Weston, Jr., and G. W. Flynn, J. Chem. Phys. **80**, 4071 (1984).
[17] C. F. Wood, G. W. Flynn, and R. E. Weston, Jr., J. Chem. Phys. **77**, 4776 (1982).
[18] C. A. Wight and S. R. Leone, J. Chem. Phys. **78**, 4875 (1983).
[19] C. A. Wight and S. R. Leone, J. Chem. Phys. **79**, 4823 (1983).
[20] J. O. Chu, G. W. Flynn, and R. E. Weston, Jr., J. Chem. Phys. **78**, 2990 (1983).
[21] C. R. Quick, Jr. and D. S. Moore, J. Chem. Phys. **79**, 759 (1983).
[22] C. A. Wight, D. J. Donaldson, and S. R. Leone, J. Chem. Phys. **83**, 660 (1985).
[23] K. Kleinermanns and J. Wolfrum, J. Chem. Phys. **80**, 1446 (1984).
[24] G. K. Chawla, G. C. McBane, P. L. Houston, and G. C. Schatz, J. Chem. Phys. **88**, 5481 (1988).
[25] J. O. Chu, C. F. Wood, G. W. Flynn, and R. E. Weston, Jr., J. Chem. Phys. **81**, 5533 (1984).
[26] J. A. O'Neill, J. Y. Cai, G. W. Flynn, and R. E. Weston, Jr., J. Chem. Phys. **84**, 50 (1986).
[27] J. O. Chu, G. W. Flynn, and R. E. Weston, Jr., J. Chem. Phys. **80**, 1703 (1984).
[28] T. H. Dunning, J. Chem. Phys. **73**, 2304 (1980).
[29] L. C. Geiger and G. C. Schatz, J. Phys. Chem. **88**, 214 (1984).
[30] J. N. Murrell and J. A. Rodriguez, J. Mol. Struct. (Theochem) **139**, 267 (1986).
[31] L. C. Geiger, G. C. Schatz, and L. B. Harding, Chem. Phys. Lett. **114**, 520 (1985).
[32] H. Romanowski, K.-T. Lee, J. M. Bowman, and L. B. Harding, J. Chem. Phys. **84**, 4888 (1986).
[33] K.-T. Lee and J. M. Bowman, J. Chem. Phys. **85**, 6225 (1986); **86**, 215 (1987).
[34] B. Gazdy, J. M. Bowman, and Q. Sun, Chem. Phys. Lett. **148**, 512 (1988).
[35] B. Gazdy and J. M. Bowman, Phys. Rev. A. **36**, 3083 (1987).
[36] L. C. Geiger, G. C. Schatz, and B. C. Garrett, in *Resonances in Electron-Molecule Scattering, van der Waals Complexes, and Reactive Chemical Dynamics*, edited by D. G. Truhlar (American Chemical Society, Washington, D.C., 1984), Chap. 22.
[37] Y. H. Kim and D. A. Micha, J. Chem. Phys. **90**, 5486 (1989).
[38] K. Watanabe and A. S. Jursa, J. Chem. Phys. **41**, 1650 (1964).
[39] R. T. Hodgson, P. P. Sorokin, and J. J. Wynne, Phys. Rev. Lett. **32**, 343 (1974).
[40] S. C. Wallace and Zdasiuk, Appl. Phys. Lett. **28**, 449 (1976).
[41] P. P. Hermann, P. E. La Rocque, R. H. Lipson, W. Jamroz, and B. P. Stoicheff, Can. J. Phys. **63**, 1581 (1985).
[42] I. Burak, J. W. Hepburn, N. Sivakumar, G. E. Hall, G. K. Chawla, and P. L. Houston, J. Chem. Phys. **86**, 1258 (1987).

[43] N. Sivakumar, Ph.D. thesis, Cornell University, 1986.
[44] J. Rice, G. Hoffman , and C. Wittig, J. Chem. Phys. **88**, 2841 (1988).
[45] We use the notation v,J and v'',J'' to indicate the vibrational, rotational level of CO populated by the collision, which is equal to the lower spectroscopic level probed by the laser-induced fluorescence. The notation v''',J''' gives the upper laser-induced fluorescence level, while the notation v'',J'' gives the level to which the upper level fluoresces.
[46] G. Guelachvili, D. de Villeneuve, R. Farrenq, W. Urban, and J. Verques, J. Mol. Spec. **98**, 64 (1983).
[47] A. W. Le Floch, F. Laumay, J. Rostas, R. W. Field, C. M. Brown, and K. Yoshino, J. Mol. Spec. **121**, 337 (1987).
[48] R. W. Field (unpublished results).
[49] J. T. Hougen, Nat. Bur. Std. Monogr. 115 (1970).
[50] I. M. Waller and J. W. Hepburn, J. Chem. Phys. **88**, 6658 (1988).
[51] R. D. Levine and R. B. Bernstein, Acc. Chem. Res. **7**, 393 (1974).
[52] G. N. A. Van Veen, K. A. Mohammed, T. Baller, and A. E. DeVries, Chem. Phys. **74**, 261 (1983).
[53] Z. Xu, B. Koplitz, and C. Wittig, J. Chem. Phys. **87**, 1062 (1987).
[54] X. Xie, L. Schnieder, H. Wallmeier, R. Boettner, K. H. Welge, and M. N. R. Ashfold, J. Chem. Phys. **92**, 1608 (1990).
[55] One would also expect experiments at 1.6 eV to exhibit the dramatic peak in the $v=0$ cross section at low J. We were unable to perform such experiments at 1.6 eV because the signal to-noise ratio was much smaller. Attempts to reduce the background population of low-J levels in $v=0$ by seeded expansions produced signals too weak to measure.
[56] P. Warneck, Z. Naturforsch. **A29**, 350 (1974).
[57] D. E. Milligan and M. E. Jacox, J. Chem. Phys. **51**, 277 (1969).
[58] J. A. O'Neill, C. X. Wang, J. Y. Cai, G. W. Flynn and R. E. Weston, J. Chem. Phys. **88**, 6240 (1988).
[59] C. T. Wickham-Jones, H. T. Williams, and C. J. S. M. Simpson, J. Chem. Phys. **87**, 5294 (1987).
[60] A. D. Sappey and D. R. Crosley (private communication).
[61] X. Zhao, G. W. Adamson, and R. W. Field (private communication).